Research Square

Preprints are preliminary reports that have not undergone peer review.
They should not be considered conclusive, used to inform clinical practice,
or referenced by the media as validated information.

Osteocytic Connexin 43 Deficiency Attenuates Disuse-Induced Epiphyseal Bone Loss in Female Mice via a β-catenin–Dependent Mechanism

Gabriel A. Hoppock
Virginia Commonwealth University, Department of Biomedical Engineering
Evan G. Buettmann
Virginia Commonwealth University, Department of Biomedical Engineering
Galen M. Goldscheitter
Virginia Commonwealth University, Department of Biomedical Engineering
Jessica R. Williamson
Virginia Commonwealth University, Department of Biomedical Engineering
Jolene J. Windle
Virginia Commonwealth University, Department Cellular, Molecular and Genetic Medicine
Henry J. Donahue
hjdonahue@vcu.edu

Virginia Commonwealth University, Department of Biomedical Engineering

Research Article

Keywords:

Posted Date: November 19th, 2026

DOI: https://doi.org/10.21203/rs.3.rs-11542304/v1

License: This work is licensed under a Creative Commons Attribution 4.0 International License.
Read Full License

Additional Declarations: No competing interests reported.

Abstract

Gap junctional intercellular communication (GJIC) and WNT/β-catenin signaling regulate skeletal development, homeostasis, and mechanotransduction. Deletion of connexin 43 (Cx43; Gja1) in Col1-expressing cells reduces cortical bone mass but attenuates disuse-induced bone loss. Similarly, β-catenin haploinsufficiency produces sexually dimorphic reductions in cortical bone and attenuates disuse-induced loss. Whether these effects reflect osteocytic versus osteoblastic Cx43, and whether Cx43 acts through β-catenin, remains unclear. We hypothesized that osteocyte-specific Cx43 deficiency reduces cortical bone mass but protects trabecular bone from unloading through a β-catenin–dependent mechanism.

Using Dmp1-Cre, we generated osteocyte-specific Cx43 knockout ($Cx43^{\Delta OCY}$), β-catenin haploinsufficient (β-catΔOCY), and double-mutant (Cx43ΔOCY/$\beta\text{-cat}^{\Delta OCY}$) mice. Skeletally mature males and females (24–28 weeks) underwent 3 weeks of hindlimb suspension (HLS) or remained ambulatory. Longitudinal microCT assessed distal femoral epiphyseal trabecular and mid-diaphyseal cortical microarchitecture; three-point bending evaluated mechanical properties.

At baseline, male $Cx43^{\Delta OCY}$ mice had increased epiphyseal trabecular BV/TV, whereas $\beta\text{-cat}^{\Delta OCY}$ mice of both sexes had decreased BV/TV. Double mutants showed no net trabecular phenotype, suggesting opposing effects of Cx43 and β-catenin. All genotypes exhibited cortical thinning, especially males. HLS-induced epiphyseal BV/TV loss was attenuated in female $Cx43^{\Delta OCY}$ mice, but this protection was absent in males and abrogated in double-mutant females, implicating β-catenin in the sexually dimorphic response. Cortical loss occurred across genotypes and sexes. β-catenin deficiency and HLS impaired whole-bone and tissue-level mechanics more than Cx43 deficiency alone

.

Introduction

Osteocytes, terminally differentiated osteoblasts embedded within mineralized matrix, constitute the vast majority (90–95%) of bone cells and orchestrate bone remodeling by secreting factors that regulate osteoblast and osteoclast activity, including sclerostin, dickkopf-related protein 1 (DKK1), nuclear factor-kappa-B ligand (RANKL), and osteoprotegerin (OPG).[1–7] Abundant evidence supports osteocytes as the primary mechanosensors in bone that translate loading, or its absence, into remodeling signals.[8–15] Despite this, the mechanisms by which osteocytes coordinate remodeling during mechanical unloading remain incompletely defined.

Gap junctional intercellular communication (GJIC), largely mediated by Cx43 in bone, regulates bone growth, remodeling, and mechanical responsiveness.[8, 16–19] Prior studies demonstrate that Cx43 deficiency in osteoblasts/osteocytes reduces cortical structure and strength and blunts the catabolic response to unloading.[17, 19, 20] However, the osteocyte-specific role of Cx43—especially its downstream molecular partners—in these processes is unresolved.

The canonical WNT/β-catenin pathway is central to skeletal homeostasis and mechanotransduction and has been implicated in the response to unloading.[14, 21–25] Cx43 influences WNT/β-catenin target gene expression and Sost levels in vivo and sclerostin secretion in vitro [13, 26, 27], and can bind β-catenin in epithelial cells, limiting its nuclear translocation.[28–30] β-catenin haploinsufficiency shows sex-dependent effects on unloading-induced loss.[31] Direct genetic testing of Cx43–β-catenin interdependence in osteocytes during disuse has been lacking.

We hypothesized that osteocytic Cx43 deficiency would reduce cortical bone mass and attenuate disuse-induced bone loss via a WNT/β-catenin–dependent mechanism. We further posited minimal baseline trabecular effects of Cx43 loss but protection from unloading-induced trabecular loss, and that outcomes would be sexually dimorphic. Using Dmp1-Cre–driven conditional models—Cx43$^{\Delta OCY}$, β-cat$^{\Delta OCY}$, and Cx43$^{\Delta OCY}$/β-cat$^{\Delta OCY}$—we assessed baseline microarchitecture, unloading responses via hindlimb suspension (HLS), and mechanical properties in both sexes.

Methods

Transgenic mouse model

All procedures were approved by the Virginia Commonwealth University IACUC (AD10001341). Mouse strains on a C57BL/6 background included Gja1flox (Cx43; JAX #008039)[32],Ctnnb1flox (β-catenin; JAX #004152)[33], and Dmp1-Cre (JAX #023047).(35) Experimental genotypes were generated by crossing these lines to obtain Dmp1-Cre; Gja1flox/flox (Cx43$^{\Delta OCY}$), Dmp1-Cre; Ctnnb1flox/+ (β-cat$^{\Delta OCY}$), and Dmp1-Cre; Gja1flox/flox; Ctnnb1flox/+ (Cx43$^{\Delta OCY}$/β-cat$^{\Delta OCY}$). Cre-negative littermates served as wild-type controls. Breeding schemes were optimized so that all offspring were usable experimental genotypes.

Hindlimb Suspension

Skeletally mature male and female mice aged 24–28 weeks were acclimated to HLS housing for approximately two weeks prior to the experiment, as we previously described.[18, 20] Within each genotype and sex, mice were assigned to ambulatory control or HLS for three weeks (n = 8–12 per group). Littermate controls were used due to baseline wild-type differences among lines.

In Vivo Micro-Computed Tomography

In vivo micro–computed tomography (microCT) scans of the femora were acquired at baseline (day 0) and day 21 using a Skyscan 1276 system (7.0 μm voxel, 60 kV, 200 μA, 730 ms, 0.5 mm Al filter). Reconstructions were performed with CT Recon (20% beam hardening; Gaussian smoothing, sigma = 2), and volumes were oriented using anatomic landmarks in DataViewer. Trabecular bone was quantified in

a 525 μm region distal to the growth plate in the left distal femoral epiphysis, and cortical bone was analyzed in a 190 μm mid-diaphyseal region, using CT, as we previously described.[34, 35]

Mechanical testing

Left femora were stored in PBS with CaCl2 (57.3 mg/L) at − 80°C and thawed to room temperature prior to mechanical testing. Three-point bending to failure was performed with an 8 mm span at 1 mm/min with the anterior surface in tension[34]. Whole-bone outcomes, including stiffness, yield and ultimate load/displacement, and energy, were computed using custom MATLAB code.(38) Tissue-level properties, including Young's modulus, yield and ultimate stress and strain, and toughness, were estimated using local microCT-derived geometry at fracture sites [36].

Statistical Analyses

Sample sizes were determined *a priori* based on power analysis to determine significant effects based on treatment and mouse sex based on historical data of outcome means/variances from other studies with $\alpha = 0.5$ and $\beta = 0.2$.[18, 20] Data were tested for normality using the D'Agostino normality test. Statistical analyses were performed using GraphPad Prism (Version 10.0.3) software. Data are expressed as means ± standard deviation with individual data points for each column representing the total sample size. Data were analyzed using two-way analysis of variance (ANOVA) or three-way ANOVA with Sidak's post-hoc test, as appropriate. For all comparisons, $p < 0.05$ was considered significant.

Results

Cx43 Deficiency and β-catenin Deficiency Have Opposite Effects on Trabecular Bone at Baseline, While Deficiency of Both Nullifies Phenotype

At baseline in the distal femoral epiphysis, osteocyte-specific Cx43 deficiency increased BV/TV compared to littermate controls (Fig. 1A;"^ symbol significant effect of genotype"). Post-hoc analysis demonstrated significant increases in $Cx43^{\Delta OCY}$ males compared with wild-type controls, whereas $Cx43^{\Delta OCY}$ females exhibited a similar but nonsignificant upward trend. (Fig. 1A; $p < 0.005$ for males and $p > 0.05$ for females). Increases in trabecular bone with Cx43 deficiency are emphasized in representative microCT images from male mice (Fig. 1B-C). In contrast, β-catenin haploinsufficiency reduced BV/TV in both sexes relative to wild-type mice (Fig. 1D; $p < 0.05$ for females and $p < 0.0005$ for males**).** The decreases in trabecular bone with β-catenin haplo insufficiency are emphasized in representative microCT images from male mice (Fig. 1E-F). The double knockout, combining Cx43 deletion with β-catenin haploinsufficiency, did not differ from wild-type for BV/TV across sexes, consistent with opposing actions of Cx43 and β-catenin on trabecular architecture (Fig. 1G; **genotype main effect ^** $p > 0.05$). These trabecular patterns were reflected in related indices, including tissue

mineral density, trabecular number, thickness, and separation, as detailed in the supplemental data (Supplemental **Tables 1, 2 and 3**).

Cx43 Deficiency, β-catenin Deficiency, and Deficiency of Both All Result in Cortical Bone Loss

In the diaphyseal cortex at baseline, all three genotypes exhibited cortical thinning (Fig. 2A-B, E-F, **and I-J**). Both Cx43$^{\Delta OCY}$ and β-cat$^{\Delta OCY}$ mice had reduced cortical area fraction (Ct.Ar/T.Ar) and cortical thickness (Cs.Th) relative to wild-type controls, and these effects were generally more pronounced in males (Fig. 2A-B **and E-F).** The double mutant showed further reductions in Ct.Ar/T.Ar and Cs.Th in both sexes **(**Fig. 2I-J**)**, indicating that Cx43 and β-catenin are each required for maintaining cortical structure. Representative microCT images from male mice (Fig. 2C-D, G-H, **and K-L).** Values for cortical area, tissue area, and tissue mineral density are included in the supplemental data **(Supplemental Tables 1, 2, and 3).**

Cx43 Deficiency Attenuates While β-catenin Deficiency Increases the Magnitude of HLS-Induced Epiphyseal Bone Loss in a Sexually Dimorphic Manner

With HLS epiphyseal trabecular bone responded in a sex- and genotype-dependent manner. Overall, BV/TV decreased with unloading (Fig. 3A-C). Within the Cx43 model, pairwise analyses revealed significant losses in WT females, WT males, and Cx43$^{\Delta OCY}$ males with unloading. Notably, female Cx43$^{\Delta OCY}$ mice did not exhibit significant unloading-induced loss, indicating attenuation of trabecular bone loss in this group. In β-cat$^{\Delta OCY}$ mice, unloading reduced BV/TV in both sexes, with greater loss in males; however, male β-cat$^{\Delta OCY}$ mice lost less trabecular bone than male WT controls, suggesting some attenuation in males but not females. In the double knockout model, both sexes lost significant BV/TV with unloading, and the genotype- and sex-specific attenuation seen in the single deletions was absent. This loss of protection in Cx43$^{\Delta OCY}$/β-cat$^{\Delta OCY}$ females implicates β-catenin is necessary for the Cx43-dependent protective response observed in female trabecular bone. Similar patterns were observed for trabecular thickness, number, and separation. **(Supplemental Tables 4, 5, and 6**).

Diaphyseal Bone Loss Was Not Affected by Cx43 or β-catenin Deficiency

HHS induced cortical loss at the diaphysis across all genotypes (Fig. 4). The cortical area fraction decreased with unloading in each line, with effects often more pronounced in females. In the double knockout model, a genotype-by-unloading interaction suggested a reduced magnitude of loss relative to wild-type when expressed as percent change ($p = 0.0460$); however, absolute losses were similar due to baseline differences.

Cx43 Deletion has a Minimal Effect on Mechanical Properties While β-catenin Deficiency Decreases Whole-Bone and Tissue Level Material Properties

Mechanical testing corroborated the microstructural findings (Fig. 5). $Cx43^{\Delta OCY}$ mice demonstrated significant main effects of HLS and sex, with HLS decreasing the ultimate load from 3-point bending and males withstanding higher ultimate loads than females regardless of HLS or genotype (Fig. 5A; $p < 0.0001$ and $p < 0.0001$, respectively). $\beta\text{-cat}^{ht\Delta OCY}$ and $Cx43^{\Delta OCY}/\beta\text{-cat}^{ht\Delta OCY}$ mice demonstrated similar trends, but also demonstrated significant main effects of genotype, with knockouts experiencing lower ultimate loads than the wild-type mice for each line (Fig. 5B-C; $p < 0.0001$ and $p = 0.0206$, respectively). $Cx43^{\Delta OCY}/\beta\text{-cat}^{ht\Delta OCY}$ females experienced significant decreases in ultimate load due to HLS while males did not, and female $Cx43^{\Delta OCY}/\beta\text{-cat}^{ht\Delta OCY}$ mice experienced lower ultimate loads than female WT mice while males were not affected by genotype (Fig. 5C; $p = 0.0026$ and $p = 0.0121$, respectively**)**. All three phenotypes demonstrated decreases in ultimate stress due to HLS (Fig. 5D-F; $p = 0.0168$ for $Cx43^{\Delta OCY}$, $p = 0.0165$ for $\beta\text{-cat}^{ht\Delta OCY}$, and $p = 0.0006$ for $Cx43^{\Delta OCY}/\beta\text{-cat}^{ht\Delta OCY}$**)**, while only the $\beta\text{-cat}^{ht\Delta OCY}$ and $Cx43^{\Delta OCY}/\beta\text{-cat}^{ht\Delta OCY}$ lines demonstrated significant decreases in ultimate stress due to genetic knockdown (Fig. 5D-F; $p = 0.0754$ for $Cx43^{\Delta OCY}$, $p = 0.0004$ for $\beta\text{-cat}^{ht\Delta OCY}$, and $p < 0.0001$ for $Cx43^{\Delta OCY}/\beta\text{-cat}^{ht\Delta OCY}$**)**.

Discussion

This innovative study demonstrates site-specific and sexually dimorphic regulation of bone architecture and mechanoadaptation by osteocytic Cx43 and β-catenin. In epiphyseal trabecular bone, Cx43 deficiency increased BV/TV, particularly in males, whereas β-catenin deficiency reduced BV/TV in both sexes; the double mutant neutralized these opposing effects. These outcomes align with our proposed model in which Cx43 deficiency enhances β-catenin activity, consistent with prior observations of altered WNT target gene expression and sclerostin levels in Cx43-deficient osteocytes, as well as documented physical interactions between Cx43 and β-catenin in other cell types.[13, 26–30]

In the diaphyseal cortex, all three genotypes exhibited cortical thinning, indicating that both Cx43 and β-catenin are required to maintain cortical structure. The underlying mechanisms appeared to differ by genotype. $Cx43^{\Delta OCY}$ mice showed periosteal expansion with an enlarged marrow cavity, resulting in increased total area and cortical area but reduced cortical area fraction and cortical thickness, a pattern reminiscent of accelerated aging.[37, 38] In contrast, $\beta\text{-cat}^{\Delta OCY}$ mice exhibited signs consistent with increased endocortical resorption, including decreased cortical area with relatively constant total area and increased marrow area. The double mutant combined features of both, suggesting additive or intersecting roles for these pathways in compartment-specific cortical maintenance.

Unloading responses were highly context-dependent. Female $Cx43^{\Delta OCY}$ mice were protected from unloading-induced epiphyseal trabecular BV/TV loss, and this protection was eliminated when β-catenin was concurrently reduced, indicating that β-catenin is a necessary component for Cx43-mediated

mechanoprotection in female epiphyseal trabecular bone. Conversely, β-catenin deficiency attenuated trabecular loss in males but not females, echoing prior sex-specific observations.[31] These interactions were not recapitulated in the diaphyseal cortex, where unloading causedcortical bone loss across genotypes, and with enhanced cortical loss in the $Cx43^{\Delta OCY}$/$\beta\text{-cat}^{ht\Delta OCY}$ line, suggesting distinct compartmental and genotype related controls of bone loss with HLS. The mechanical data reinforced the microstructural findings, as β-catenin deficiency and unloading consistently reduced whole-bone and tissue-level performance more than Cx43 deficiency, in line with impaired periosteal expansion and increased endocortical resorption in $\beta\text{-cat}^{\Delta OCY}$ mice.

Collectively, these data support a model in which osteocytic Cx43 and β-catenin genetically interact to regulate remodeling and mechanoadaptation, with dependence on bone compartment and sex. The β-catenin dependence of the Cx43-mediated protective effect in female trabecular bone suggests a mechanistic link likely involving modulation of sclerostin and WNT signaling.

Limitations and Future Directions

Use of non-inducible Dmp1-Cre models creates baseline architectural differences that complicate absolute comparisons of unloading responses. Inducible Dmp1-CreERT2 strategies would better equalize baseline bone mass and enable more precise causal inference. Although Dmp1-Cre can have off-target activity in non-skeletal tissues[39], measured skeletal muscle Gja1 reductions were minimal in this study. Mechanistic investigation via histology and osteocyte-specific gene and protein expression was not undertaken. Future studies should examine Sost, Dkk1, WNT target genes, and direct Cx43–β-catenin interactions in osteocytes during unloading, with analyses stratified by sex.

Declarations

Funding Declaration.

This work was funded by NIH R01 AR068132 and NASA 80NSSC18K1473. Dr. Buettmann was supported by TRISH (NNX16AO69A) and NIAMS K99AR082989.

Use of artificial intelligence.

GPT-6 Luna, version GPT-6 Luna (release date: September 2026),model GPT-6 Luna, an AI assistant created by OpenAI, was used for editing the manuscript. The tool was used in a manner that does not conflict with APS ethical policies, and the authors take full responsibility for the content.

Author Contribution

G.H. made substantial contributions to the conception and design of the work; and the acquisition, analysis, or interpretation of data,drafted the work and revised it critically for important intellectual content, approved the version to be published; and agree to be accountable for all aspects of the work in

ensuring that questions related to the accuracy or integrity of any part of the work are appropriately investigated and resolved.E.B. acquisition, analysis, or interpretation of data, agree to be accountable for all aspects of the work in ensuring that questions related to the accuracy or integrity of any part of the work are appropriately investigated and resolved.G.G. acquisition, analysis, or interpretation of data, agree to be accountable for all aspects of the work in ensuring that questions related to the accuracy or integrity of any part of the work are appropriately investigated and resolved.J.W. acquisition, analysis, or interpretation of data, agree to be accountable for all aspects of the work in ensuring that questions related to the accuracy or integrity of any part of the work are appropriately investigated and resolved.H.D.made substantial contributions to the conception and design of the work; and the acquisition, analysis, or interpretation of data,drafted the work and revised it critically for important intellectual content, approved the version to be published; and agree to be accountable for all aspects of the work in ensuring that questions related to the accuracy or integrity of any part of the work are appropriately investigated and resolved.

Acknowledgement

This work was funded by NIH R01 AR068132 and NASA 80NSSC18K1473 (HJD) and TRISH (NNX16AO69A) and NIAMS K99AR082989 (EGB).

References

1. Bellido T (2014) Osteocyte-driven bone remodeling. Calcif Tissue Int 94(1):25–34 Epub 20130904. 10.1007/s00223-013-9774-y
2. Bonewald LF (2011) The amazing osteocyte. J Bone Min Res 26(2):229–238. 10.1002/jbmr.320. PubMed PMID: 21254230; PubMed Central PMCID: PMCPMC3179345
3. Bonewald LF, Johnson ML (2008) Osteocytes, mechanosensing and Wnt signaling. Bone 42(4):606–615 Epub 20080112. 10.1016/j.bone.2007.12
4. Nakashima T, Hayashi M, Fukunaga T, Kurata K, Oh-Hora M, Feng JQ et al (2011) Evidence for osteocyte regulation of bone homeostasis through RANKL expression. Nat Med 17(10):1231–1234 Epub 20110911. doi: 10.1038/nm.2452. PubMed PMID: 21909105
5. Tu X, Rhee Y, Condon KW, Bivi N, Allen MR, Dwyer D et al (2012) Sost downregulation and local Wnt signaling are required for the osteogenic response to mechanical loading. Bone 50(1):209–217 Epub 20111030. 10.1016/j.bone.2011.10.025
6. Xiong J, O'Brien CA (2012) Osteocyte RANKL: new insights into the control of bone remodeling. J Bone Min Res 27(3):499–505. 10.1002/jbmr.1547. PubMed PMID: 22354849; PubMed Central PMCID: PMCPMC3449092
7. Xiong JH, Onal M, Jilka RL, Weinstein RS, Manolagas SC, O'Brien CA (2011) Matrix-embedded cells control osteoclast formation. Nat Med 17(10):1235–U262. 10.1038/nm.2448. PubMed PMID: WOS:000296022100041

8. Jiang JX, Siller-Jackson AJ, Burra S (2007) Roles of gap junctions and hemichannels in bone cell functions and in signal transmission of mechanical stress. Front Biosci 12:1450–1462 Epub 20070101. doi: 10.2741/2159. PubMed PMID: 17127393; PubMed Central PMCID: PMCPMC1797155
9. Cowin SC (1998) On mechanosensation in bone under microgravity. Bone. ;22(5 Suppl):119S-25S. 10.1016/s8756-3282(98)00011-8. PubMed PMID: 9600767
10. Webster DJ, Schneider P, Dallas SL, Muller R (2013) Studying osteocytes within their environment. Bone 54(2):285–295 Epub 20130111. doi: 10.1016/j.bone.2013.01.004. PubMed PMID: 23318973; PubMed Central PMCID: PMCPMC3652555
11. Alford AI, Jacobs CR, Donahue HJ (2003) Oscillating fluid flow regulates gap junction communication in osteocytic MLO-Y4 cells by an ERK1/2 MAP kinase-dependent mechanism. Bone 33(1):64–70. 10.1016/s8756-3282(03)00167-4. PubMed PMID: 12919700
12. Blaber EA, Dvorochkin N, Torres ML, Yousuf R, Burns BP, Globus RK et al (2014) Mechanical unloading of bone in microgravity reduces mesenchymal and hematopoietic stem cell-mediated tissue regeneration. Stem Cell Res 13(2):181–201 Epub 20140609. 10.1016/j.scr.2014.05.005
13. Bivi N, Pacheco-Costa R, Brun LR, Murphy TR, Farlow NR, Robling AG et al (2013) Absence of Cx43 selectively from osteocytes enhances responsiveness to mechanical force in mice. J Orthop Res 31(7):1075–1081 Epub 20130311. 10.1002/jor.22341
14. Spatz JM, Wein MN, Gooi JH, Qu Y, Garr JL, Liu S et al (2015) The Wnt Inhibitor Sclerostin Is Up-regulated by Mechanical Unloading in Osteocytes in Vitro. J Biol Chem 290(27):16744–16758 Epub 20150507. 10.1074/jbc.M114.628313
15. Tatsumi S, Ishii K, Amizuka N, Li M, Kobayashi T, Kohno K et al (2007) Targeted ablation of osteocytes induces osteoporosis with defective mechanotransduction. Cell Metab 5(6):464–475. 10.1016/j.cmet.2007.05.001. PubMed PMID: 17550781
16. Civitelli R, Beyer EC, Warlow PM, Robertson AJ, Geist ST, Steinberg TH (1993) Connexin43 mediates direct intercellular communication in human osteoblastic cell networks. J Clin Invest 91(5):1888–1896. 10.1172/JCI116406. PubMed PMID: 8387535; PubMed Central PMCID: PMCPMC288182
17. Grimston SK, Goldberg DB, Watkins M, Brodt MD, Silva MJ, Civitelli R (2011) Connexin43 deficiency reduces the sensitivity of cortical bone to the effects of muscle paralysis. J Bone Min Res 26(9):2151–2160. 10.1002/jbmr.425. PubMed PMID: 21590735; PubMed Central PMCID: PMCPMC3306012
18. Lloyd SA, Lewis GS, Zhang Y, Paul EM, Donahue HJ (2012) Connexin 43 deficiency attenuates loss of trabecular bone and prevents suppression of cortical bone formation during unloading. J Bone Min Res 27(11):2359–2372. 10.1002/jbmr.1687. PubMed PMID: 22714552; PubMed Central PMCID: PMCPMC3683470
19. Zhao D, Liu R, Li G, Chen M, Shang P, Yang H et al (2020) Connexin 43 Channels in Osteocytes Regulate Bone Responses to Mechanical Unloading. Front Physiol 11:299 Epub 20200331. 10.3389/fphys.2020.00299

20. Lloyd SA, Loiselle AE, Zhang Y, Donahue HJ (2013) Connexin 43 deficiency desensitizes bone to the effects of mechanical unloading through modulation of both arms of bone remodeling. Bone 57(1):76–83 Epub 20130724. 10.1016/j.bone.2013.07.022
21. Robling AG, Niziolek PJ, Baldridge LA, Condon KW, Allen MR, Alam I et al (2008) Mechanical stimulation of bone in vivo reduces osteocyte expression of Sost/sclerostin. J Biol Chem 283(9):5866–5875 Epub 20071217. 10.1074/jbc.M705092200
22. Holguin N, Brodt MD, Silva MJ (2016) Activation of Wnt Signaling by Mechanical Loading Is Impaired in the Bone of Old Mice. J Bone Min Res 31(12):2215–2226 Epub 20160907. 10.1002/jbmr.2900
23. Lawson LY, Brodt MD, Migotsky N, Chermside-Scabbo CJ, Palaniappan R, Silva MJ (2022) Osteoblast-Specific Wnt Secretion Is Required for Skeletal Homeostasis and Loading-Induced Bone Formation in Adult Mice. J Bone Min Res 37(1):108–120 Epub 20211011. 10.1002/jbmr.4445
24. Tu X, Delgado-Calle J, Condon KW, Maycas M, Zhang H, Carlesso N et al (2015) Osteocytes mediate the anabolic actions of canonical Wnt/beta-catenin signaling in bone. Proc Natl Acad Sci U S A 112(5):E478–E486 Epub 20150120. 10.1073/pnas.1409857112
25. Loiselle AE, Lloyd SA, Paul EM, Lewis GS, Donahue HJ (2013) Inhibition of GSK-3beta rescues the impairments in bone formation and mechanical properties associated with fracture healing in osteoblast selective connexin 43 deficient mice. PLoS ONE 8(11):e81399 Epub 20131108. 10.1371/journal.pone.0081399
26. Bivi N, Condon KW, Allen MR, Farlow N, Passeri G, Brun LR et al (2012) Cell autonomous requirement of connexin 43 for osteocyte survival: consequences for endocortical resorption and periosteal bone formation. J Bone Min Res 27(2):374–389 PubMed PMID: 22028311; PubMed Central PMCID: PMCPMC3271138
27. Hoppock GA, Buettmann EG, Denisco JA, Goldscheitter GM, Condyles SN, Juhl, OJt et al (2023) Connexin 43 and cell culture substrate differentially regulate OCY454 osteocytic differentiation and signaling to primary bone cells. Am J Physiol Cell Physiol 325(4):C907–C20 PubMed PMID: 37602413; PubMed Central PMCID: PMCPMC10635658
28. Ai Z, Fischer A, Spray DC, Brown AM, Fishman GI (2000) Wnt-1 regulation of connexin43 in cardiac myocytes. J Clin Invest 105(2):161–171 doi: 10.1172/JCI7798. PubMed PMID: 10642594; PubMed Central PMCID: PMCPMC377428
29. Dbouk HA, Mroue RM, El-Sabban ME, Talhouk RS (2009) Connexins: a myriad of functions extending beyond assembly of gap junction channels. Cell Commun Signal 7:4 Epub 20090312. 10.1186/1478-811X-7-4
30. Talhouk RS, Mroue R, Mokalled M, Abi-Mosleh L, Nehme R, Ismail A et al (2008) Heterocellular interaction enhances recruitment of alpha and beta-catenins and ZO-2 into functional gap-junction complexes and induces gap junction-dependant differentiation of mammary epithelial cells. Exp Cell Res 314(18):3275–3291 Epub 20080808. 10.1016/j.yexcr.2008.07.030
31. Maurel DB, Duan P, Farr J, Cheng AL, Johnson ML, Bonewald LF (2016) Beta-Catenin Haplo Insufficient Male Mice Do Not Lose Bone in Response to Hindlimb Unloading. PLoS ONE

11(7):e0158381 Epub 20160713. 10.1371/journal.pone.0158381

32. Liao Y, Day KH, Damon DN, Duling BR (2001) Endothelial cell-specific knockout of connexin 43 causes hypotension and bradycardia in mice. Proc Natl Acad Sci U S A 98(17):9989–9994 Epub 20010731. 10.1073/pnas.171305298
33. Brault V, Moore R, Kutsch S, Ishibashi M, Rowitch DH, McMahon AP et al (2001) Inactivation of the beta-catenin gene by Wnt1-Cre-mediated deletion results in dramatic brain malformation and failure of craniofacial development. Development 128(8):1253–1264. 10.1242/dev.128.8.1253. PubMed PMID: 11262227
34. Friedman MA, Zhang Y, Wayne JS, Farber CR, Donahue HJ (2019) Single limb immobilization model for bone loss from unloading. J Biomech 83:181–189 PubMed PMID: 30551918
35. Buettmann EG, DeNapoli RC, Abraham LB, Denisco JA, Lorenz MR, Friedman MA et al (2023) Reambulation following hindlimb unloading attenuates disuse-induced changes in murine fracture healing. Bone 172:116748 Epub 20230330. 10.1016/j.bone.2023.116748
36. Turner CH, Burr DB (1993) Basic biomechanical measurements of bone: a tutorial. Bone. ;14(4):595–608. 10.1016/8756-3282(93)90081-k. PubMed PMID: 8274302
37. Glatt V, Canalis E, Stadmeyer L, Bouxsein ML (2007) Age-related changes in trabecular architecture differ in female and male C57BL/6J mice. J Bone Min Res 22(8):1197–1207. 10.1359/jbmr.070507. PubMed PMID: 17488199
38. Buettmann EG, Goldscheitter GM, Hoppock GA, Friedman MA, Suva LJ, Donahue HJ (2022) Similarities Between Disuse and Age-Induced Bone Loss. J Bone Min Res 37(8):1417–1434 Epub 20220728. 10.1002/jbmr.4643
39. Dallas SL, Xie Y, Shiflett LA, Ueki Y (2018) Mouse Cre Models for the Study of Bone Diseases. Curr Osteoporos Rep 16(4):466–477. 10.1007/s11914-018-0455-7. PubMed PMID: 29934753; PubMed Central PMCID: PMCPMC6397767

Figures

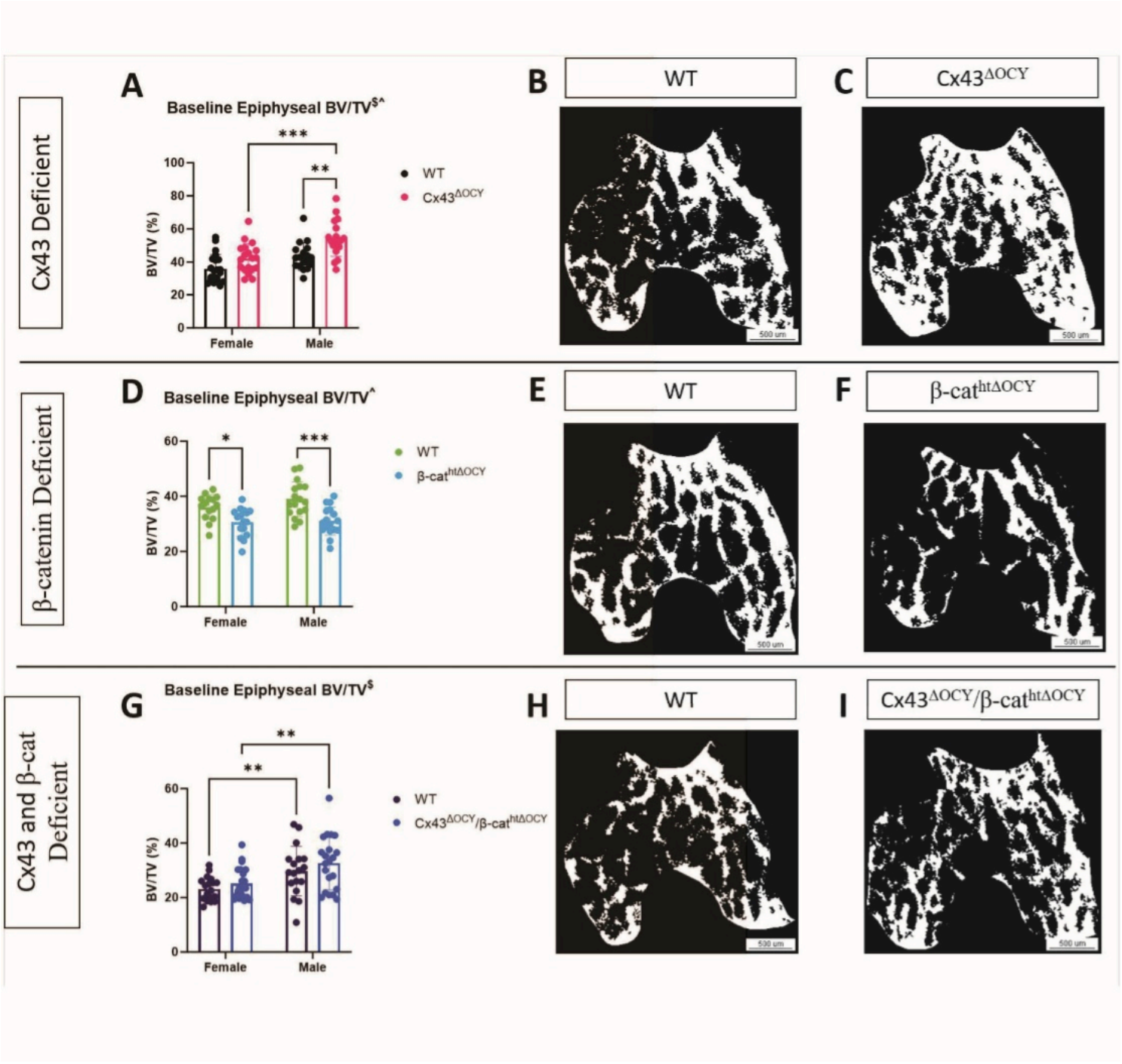


Figure 1

Cx43 deficiency increases epiphyseal BV/TV in males, whereas β-catenin deficiency decreases BV/TV in both sexes. Panels A–C compare Cx43$^{\Delta OCY}$ with wild-type. Panels D–F compare β-cat$^{\Delta OCY}$ with wild-type. Panels G–I compare Cx43$^{\Delta OCY}$/β-cat$^{\Delta OCY}$ with wild-type. Symbols indicate main effects and significance: $ main effect of sex; ^ main effect of genotype; * $p < 0.05$; ** $p < 0.005$; *** $p < 0.0005$.

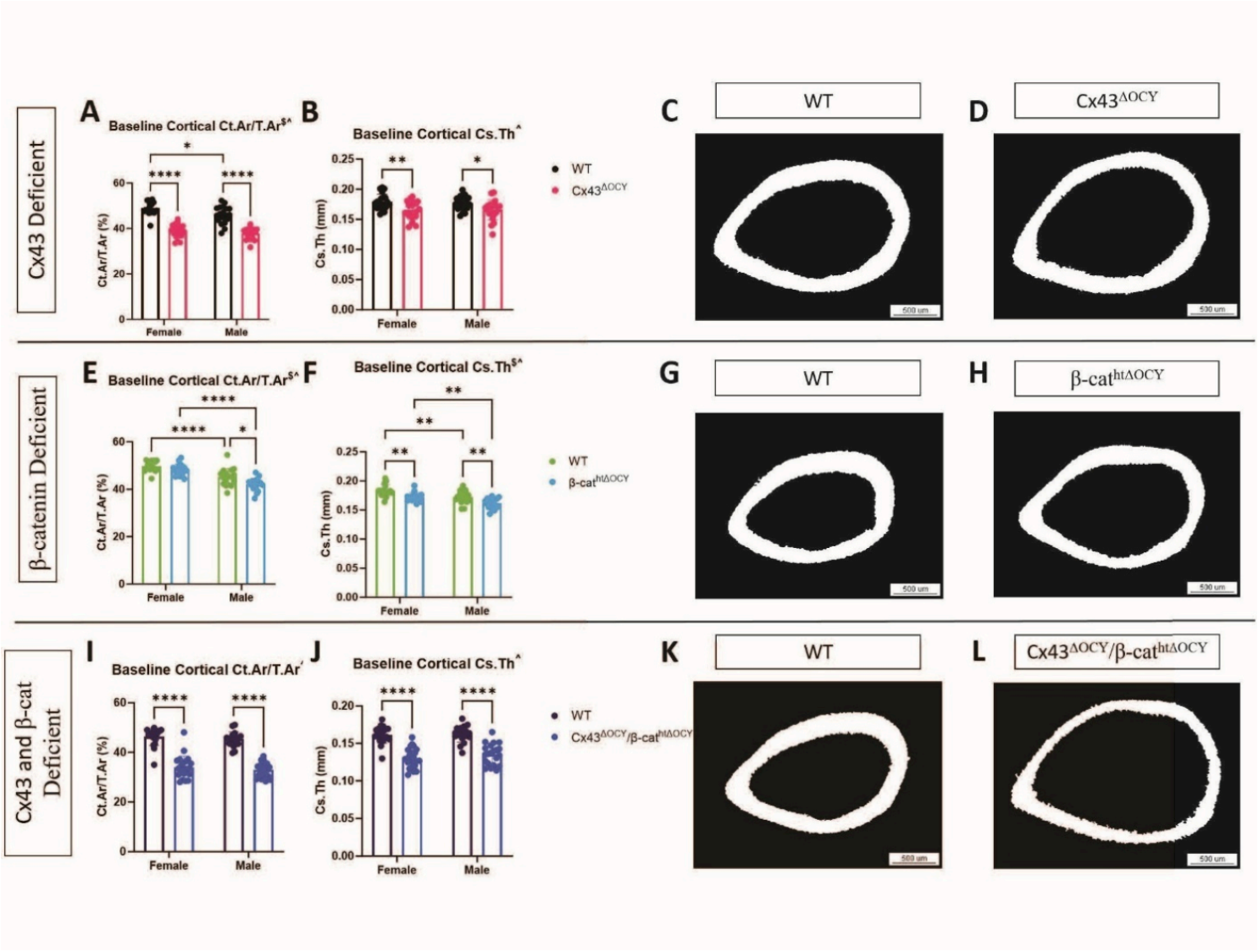


Figure 2

All three genotypes exhibit cortical thinning at baseline. Panels A–D show Cx43$^{\Delta OCY}$ versus wild-type. Panels E–H show β-cat$^{\Delta OCY}$ versus wild-type. Panels I–L show Cx43$^{\Delta OCY}$/β-cat$^{\Delta OCY}$ versus wild-type. Symbols follow Figure 1; **** $p < 0.0001$.

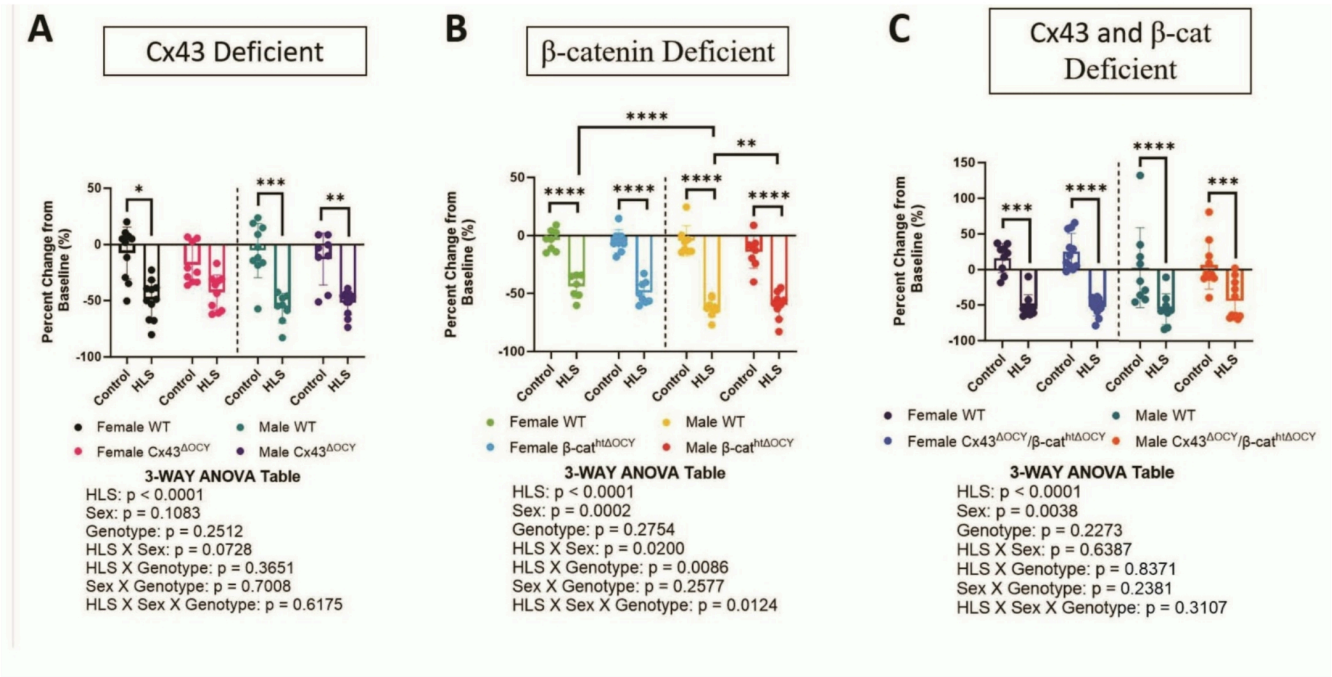


Figure 3

Female Cx43$^{\Delta OCY}$ mice show attenuated HLS-induced epiphyseal BV/TV loss; this attenuation is absent in double knockouts. Percent change from baseline is presented for Cx43$^{\Delta OCY}$ (A), β-cat$^{\Delta OCY}$ (B), and Cx43$^{\Delta OCY}$/β-cat$^{\Delta OCY}$ (C). Significance: * p < 0.05; ** p < 0.005; *** p < 0.0005; **** p < 0.0001.

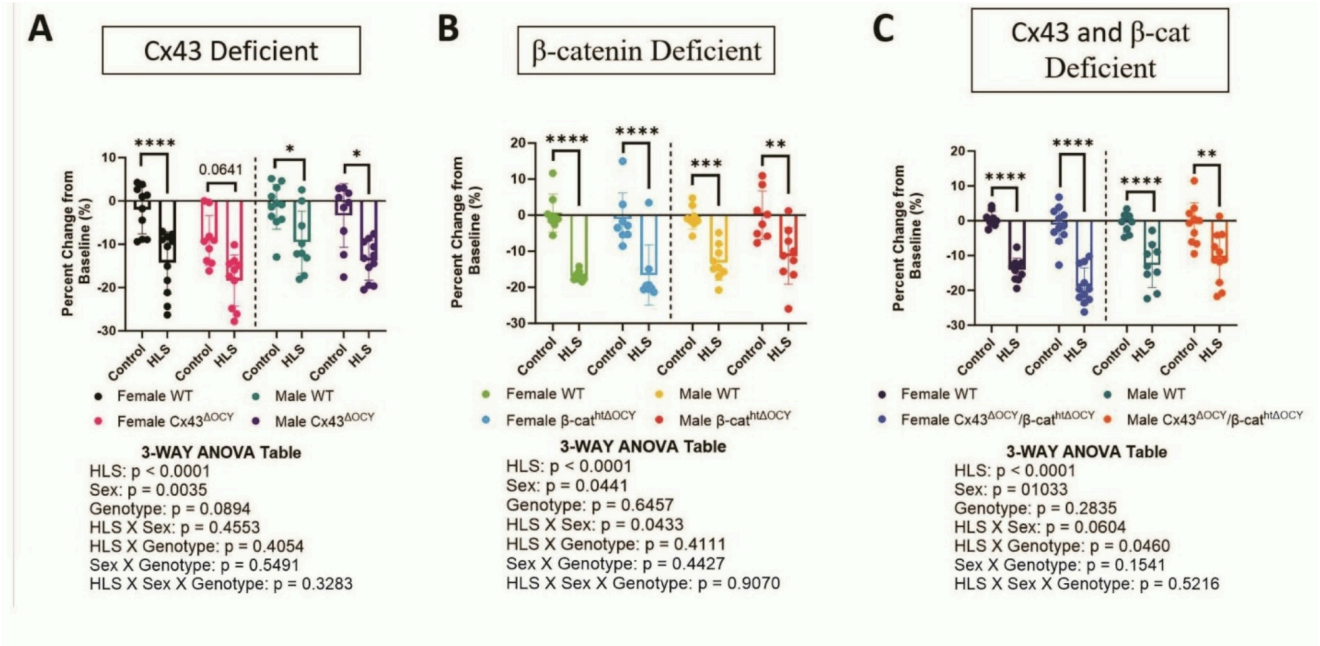


Figure 4

HLS induces diaphyseal cortical loss across genotypes. Percent change from baseline of Ct.Ar/T.Ar is shown for Cx43$^{\Delta OCY}$ (A), β-cat$^{\Delta OCY}$ (B), and Cx43$^{\Delta OCY}$/β-cat$^{\Delta OCY}$ (C), with symbols as in Figure 3.

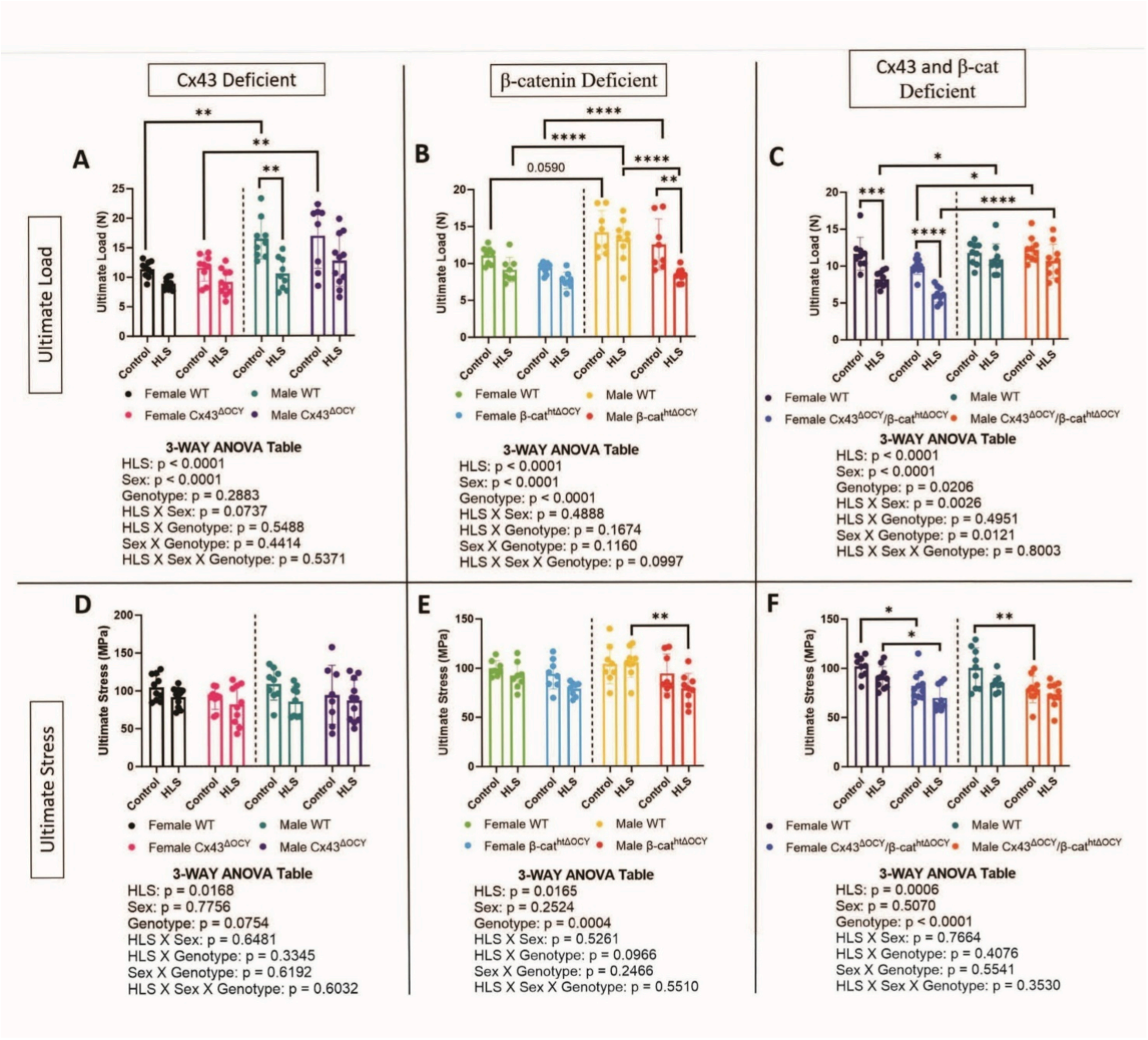


Figure 5

HLS and β-catenin deficiency impair whole-bone and tissue-level mechanics. Ultimate load (A–C) and ultimate stress (D–F) are shown for the three lines. Significant main effects include unloading and sex for all, and genotype for β-cat$^{\Delta OCY}$ and Cx43$^{\Delta OCY}$/β-cat$^{\Delta OCY}$. Interactions are noted for Cx43$^{\Delta OCY}$/β-cat$^{\Delta OCY}$.

Supplementary Files

This is a list of supplementary files associated with this preprint. Click to download.

- Supplementarytables.pdf